Nonlinear Phenomena in Complex Systems, vol. **25**, no. 3 (2022), pp. 229 - 244

Polarization Properties of the Electrically Controlled Twist-Planar Liquid Crystal Diffraction Structure

Elena Melnikova,* Ihar Stashkevich, Irina Rushnova, and Alexei Tolstik
Faculty of Physics, Belarusian State University,
4 Nezalezhnasti Ave., 220030 Minsk, BELARUS

Sergei Timofeev
A. N. Sevchenko Institute of Applied Physical Problems of the Belarusian State University,
7 Kurchatov St., 220045, Minsk, BELARUS
(Received 06 July, 2022)

The properties of the designed anisotropic diffraction structures based on the spatially structured electrically-controlled liquid crystal elements have been studied. Such a diffraction structure represents interchanging layers of a nematic liquid crystal with planar and twist orientations of the director. It is formed when a photosensitive polymer is subjected to the effect of polarized ultraviolet radiation through a photolithographic mask. It is shown that increase in voltages leads to transformations of the liquid crystal structure. At minor voltages the diffraction structure may be considered as two amplitude gratings with orthogonal polarizations at the output. At the voltage associated with the broken Mauguin condition (optical threshold of the twist effect) the amplitude-to-phase transformation of the diffraction structure takes place and its diffraction efficiency becomes higher. The proposed theoretical model enables one to explain the relationship between diffraction characteristics of a diffraction element and applied voltage or polarization of light. A good agreement of theoretical and experimental results is demonstrated.

PACS numbers: 42.70.Df, 42.79.-e, 42.25.Lc, 42.25.Ja, 42.70.Fx
Keywords: liquid crystal, anisotropic phase grating, diffraction efficiency, polarization influence
DOI: https://doi.org/10.33581/1561-4085-2022-25-3-229-244

1. Introduction

At the present time liquid crystals (LC) hold a firm place in the production of recording, displaying, and information processing devices [1, 2]. LC media are used as functional materials for the creation of competitive systems for the control of light beams: spatial light modulators, optical filters, switches, diffraction elements, tunable lenses, singular optics elements, and the like [3-6]. A choice of liquid crystals offers much promise due to their unique properties including high sensitivity to the effects of external (electric, thermal, optical) fields which enable one to control optical anisotropy. Special attention is given to the development of LC-based diffraction optical elements which make possible the spatial control, multiplexing, transformations of the light field polarization and phase [7-12]. A great interest to LC diffraction gratings is associated with such advantages as low voltages and minor energy consumption, wide working range of wave lengths, long operating time. LC gratings are produced with the use of advanced thin-film technologies; their control is realized using the latest achievements in microelectronics [13, 14]. The formation of the locally-inhomogeneous LC distribution on the conductive surface may be attained by means of the electrodes having special configuration, of such methods as photolithography, microrubbing of orienting films, scribing with a needle of an atomic-force microscope, photoalignment of light-sensitive materials (polymers, azo polymers, azo dyes) [15, 16]. Among the advantages of the photoalignment method are the following: possibility of forming

*E-mail: Melnikova@bsu.by

LC structures with the desired azimuthal director orientation in the selected region; formation of the required inclination angles of LC molecules to the substrate; control over the energy of cohesion with the orienting layer [17, 18]. Owing to the contactless photoalignment method, it is possible to locally control the LC director distribution on the surface having a spatial resolution on the order of several microns. As photoorientants used to set the boundary conditions for the LC director distribution, photopolymers still remain at the leading positions because they are characterized by high azimuthal energies of cohesion with LC materials, film thickness homogeneity, optical transparency, uniformity of orientational properties [19, 20]. The patterned photoalignment technology of LC materials that has already shown great advances is now an optimal solution for the creation of one-, two- , and three-dimensional optical diffraction elements which offer the control over the spatial, phase or polarization characteristics of light fields [21-28]. Of various topologies for the initial LC director orientation in the interchanging domains of diffraction elements most interesting are the structures with a periodic variation of twist- and planar-oriented domains [29 - 34]. Just this topology of the LC director orientation offers a high value of the first-order diffraction efficiency [34]. In [33] the dependence between diffraction efficiency and control voltage has been studied experimentally for two orthogonal polarization modes of one- and two-dimensional LC gratings with a twist-planar orientation in the neighboring domains. Qualitatively, the controlled diffraction at such a structure may be explained by the transformation from the amplitude grating (within a low electric field) to the phase one (within a high electric field). Based on the model considered in this paper, it has been concluded that the diffraction efficiency is independent of the incident-light polarization direction in low- and high-field regions of the external control electric field. However, the authors have demonstrated that the diffraction efficiency - voltage dependence is sensitive to polarization.

In the process of work forming the basis for the present paper the authors have used the LC director photoalignment method to develop the anisotropic electrically-controlled diffraction structures with a twist-planar orientation of the director. Experimental studies of their diffraction and polarization characteristics have revealed that at these structures diffraction is dependent on polarization. This is explained using a theoretical model based on calculations of polar and azimuthal angles for the LC director orientation in planar and twist domains as a function of the control voltage. The dependence between diffraction efficiency and voltage for two orthogonal polarization modes has been analyzed theoretically. The dependence between the diffracted-radiation polarization state and the control voltage has been analyzed using the Jones matrix method. A good agreement of the theoretical and experimental results has been demonstrated.

2. LC diffraction element. Technology

The proposed diffraction optical element has been developed using the technology aimed at the formation of spatial modulation of the LC director orientation by means of patterned photoalignment. The diffraction structure was formed when a photosensitive polymer was exposed to polarized ultraviolet radiation through a photolithographic mask [35, 36]. To study polarization features of the diffraction efficiency control voltage dependence in a nematic liquid crystal (NLC), a diffraction grating with a constant spatial frequency was formed. The LC cell schematic diagram is shown in Fig. 1.

The initial LC director topology of the LC diffraction element represents periodically interchanging twist and planar domains in a NLC layer. The diffraction LC element under study comprises two glass plates with transparent electrodes of indium oxide. The LC layer thickness d comes to 20 μm. The photosensitive polymeric layer was deposited on the electrode surfaces

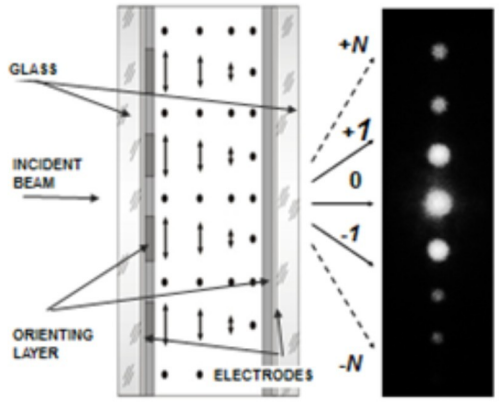

FIG. 1: Schematic diagram for the electrically controlled LC element.

to be expose to polarized ultraviolet radiation. The photopolymer on one of the substrates was illuminated by spatially-homogeneous radiation, whereas for the second substrate the amplitude grating was used. We have used a positive nematic crystal (NLC 1289) on the basis of cyanobiphenyls and Demuth esters developed at the Research Institute for Applied Physical Problems of the Belarusian State University (BSU). The refractive index at the probing radiation wavelength 633 nm for an extraordinary wave was $n_e = 1.69$, for an ordinary wave it was $n_o = 1.53$. The orienting layer was made of the polymer developed at the Physical Optics and Applied Informatics Department (BSU) [37].

Fig. 2 presents the technology used for the development of a diffraction NLC structure with interchanging twist and planar domains. To set the initial orientation topology in LC, the photoorientant layer on one of the substrates was subjected to two-stage irradiation. At the first stage the photopolymer was exposed to linearly-polarized UV radiation ($\lambda = 254\,nm$) through the quartz amplitude grating ($\Lambda = 20\,\mu$m) that lead to polymeric linkage in the irradiated domains.

At the second stage the polarization direction of UV radiation within the substrate plane was at an angle of 90°, leading to irradiation of the whole surface. Irreversibility of the linkage process results in the formation of periodic domains with orthogonal directions of the induced surface anisotropy for the photolinking orientation. The second substrate was uniformly irradiated by linearly polarized radiation over the whole surface. The prepared substrates were glued with regard to the preset gap (20 μm) of the planar capillary filled with NLC. In this way interchanging of twist- and planar-oriented LC director domains was realized within the plane of the LC element.

Fig. 3 presents polarization photomicrographs, for the periodic structure featuring the multiple-domain LC director orientation, which were made at crossed polarizers (a) and also the laser-radiation diffraction pattern of the LC element (b) for different voltages. As seen, the initial profile of the formed diffraction structure is close to the rectangular one offering high-order diffraction, and the intensity distribution of radiation at diffraction of different orders is dependent on the applied voltage.

3. LC element diffraction efficiency. Experimental results

In this section consideration is given to analysis of the experimental results obtained in the process of measuring the LC element diffraction efficiency as a function of the control voltage amplitude. The two mutually orthogonal polarization states of radiation incident on the element have been considered.

When the E-vector of a light wave was parallel to the grating grooves, polarization was vertical, when it was orthogonal to the grooves, polarization was horizontal. Experimental curves for diffraction efficiency as a function of voltage for two polarization orientations are given in Fig. 4.

It is seen that the initial diffraction efficiencies at the voltage U = 0 V for both polarization modes in directions of zero- (directly transmitted radiation) and first-order diffractions

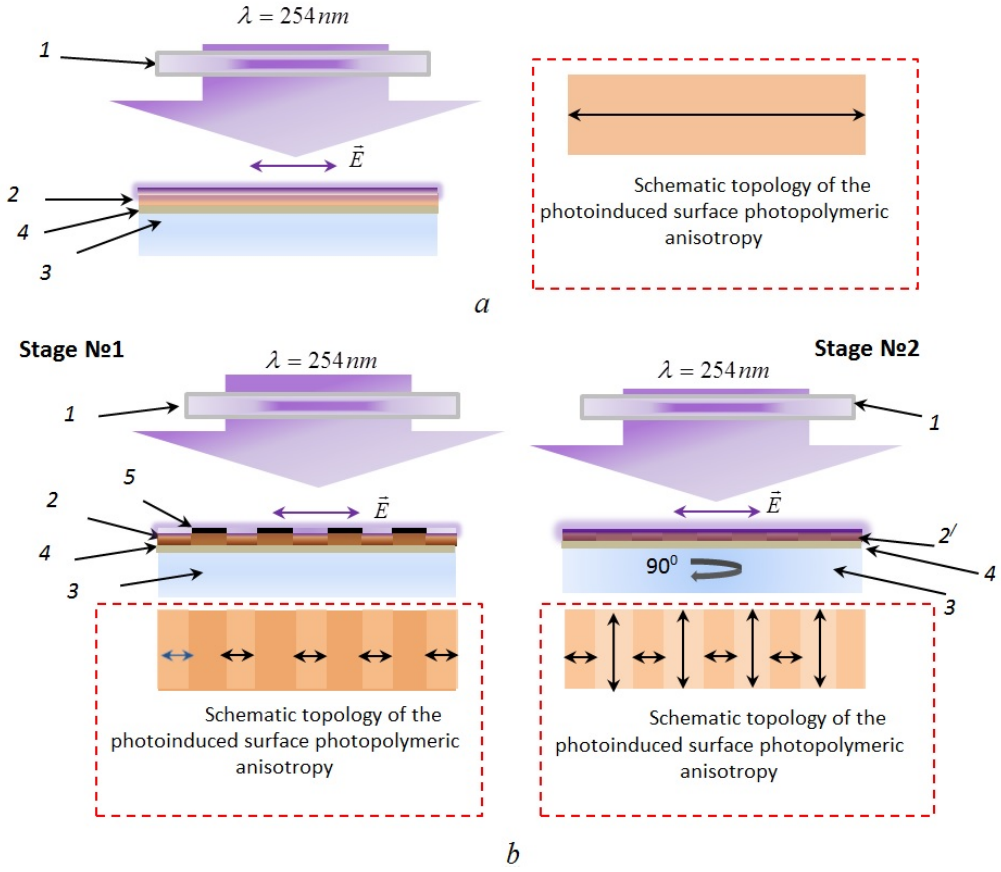

FIG. 2: (color online) Substrate preparation method: a – preparation of substrate No. 1 for the formation of the uniform surface anisotropy of the polymeric layer, b – preparation of substrate No. 2 for the formation of microstructured two-domain surface anisotropy of the photopolymeric layer. 1 – WG – polarizer, 2, 2' – photopolymeric layer B-15, 3 – glass substrate, 4 – transparent electrode (ITO), 5 – amplitude quartz transparency ($\Lambda = 20\,\mu$m).

come to $\eta_0 = 50$ % and $\eta_1 = 20\%$, respectively. When the external voltage is growing up to the value corresponding to the broken Mauguin condition (optical threshold of the twist effect) [38], the diffraction structure is transformed from an amplitude to the phase one that is characterized by a higher diffraction efficiency. Maximal efficiency for the first-order diffraction was as high as 28%, approaching the limiting diffraction-efficiency value for a thin sinusoidal phase grating.

Further increase in the amplitude of the control voltage across the LC element results in reorientation of the LC director, whereas molecules in the twist and planar domains tend to homeotropic orientation. For voltages higher than 10 V, the diffraction efficiency approaches zero pointing to the fact that the diffraction LC structure is broken. It should be noted, diffraction efficiencies for orthogonal polarizations of a light beam at various voltages reveal a slight difference of degree.

4. Diffraction efficiency of LC element. Numerical simulation

To simulate numerically the dependence between diffraction efficiency and voltage, let

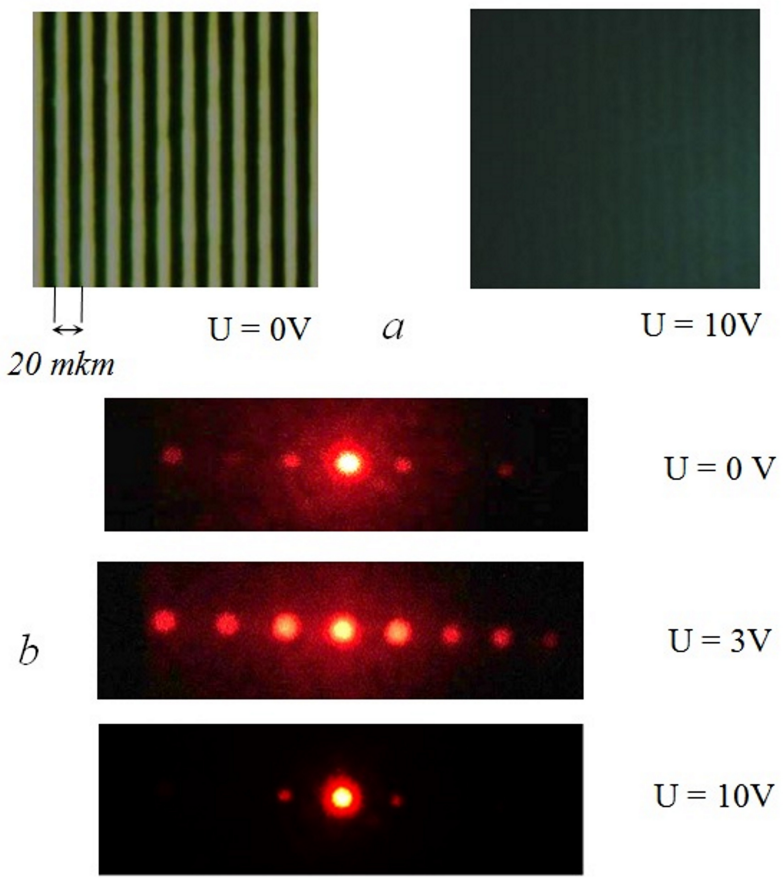

FIG. 3: (color online) Polarization photomicrographs, for the periodic structure featuring the multiple-domain LC director orientation.

us specify the LC director orientation in the rectangular coordinate system XYZ (Fig. 5).

The initial LC-director orientation in both domains is lying within the XY plane. When the control voltage is applied, a planar domain reveals the S -effect characterized by the polar angle θ (Fig.5, a). Untwisting of the director in a twist domain under the effect of an electric field is realized with the development of S-, B- , and T-effects, orientation of the director in a twist domain being determined by the polar angle θ and the azimuthal angle ϕ (Fig.5, b).

For a qualitative description of the dependence between diffraction efficiency and control voltage, let us select four operating modes of a diffraction optical element (DOE) with respect to the character of NLC deformation in twist domains under an electric field. Isolation of operating modes of the element according to the operating voltage enables one to explain qualitatively the diffraction features of linearly polarized light. Consider each of the modes in Fig.6.

4.1. Twist structure: Mauguin mode

The operating mode associated with a nondeformed twist structure (Fig.6, a) defines a character of operation for the diffraction LC element as diffraction of linearly polarized light from two independent amplitude gratings. For

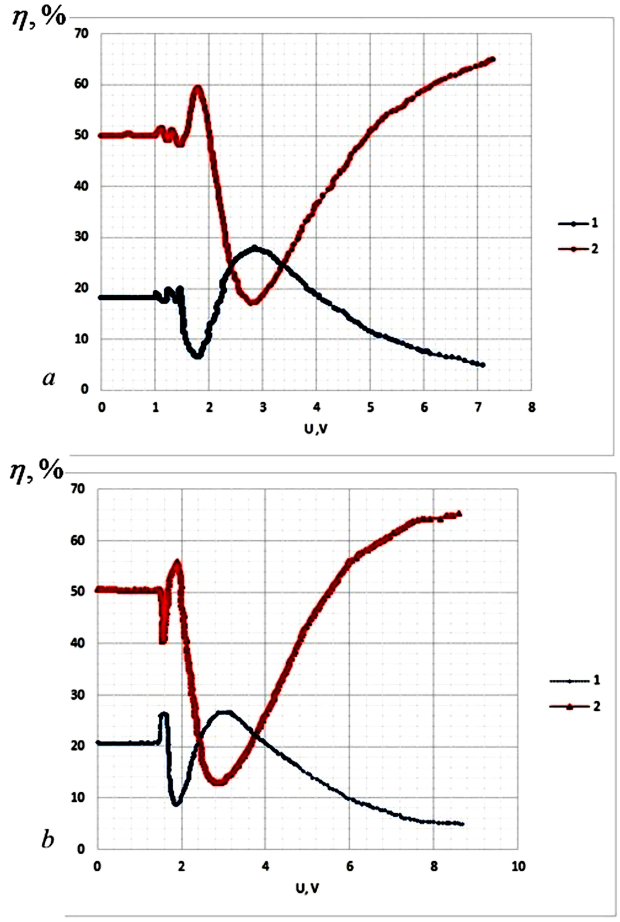

FIG. 4: (color online) Experimental curves for diffraction efficiency as a function of voltage at vertical (a) and horizontal (b) polarizations of incident radiation (1 - zero order, 2 - first-order diffraction).

better understanding, see Fig. 7 showing a schematic model of diffraction.

In Fig. 7a, it is seen that within the period of the diffraction structure Λ, there are two LC domains with planar and twist orientations of the director which enable interchanging of mutually orthogonal orientations of the E-plane for a linearly polarized electromagnetic wave at the output of the LC element. In the region of the LC director twist orientation the polarization plane rotates by an angle of 90° (Fig.7, b). The polarization state is invariable for the domain with a planar orientation of LC (Fig.7, c).

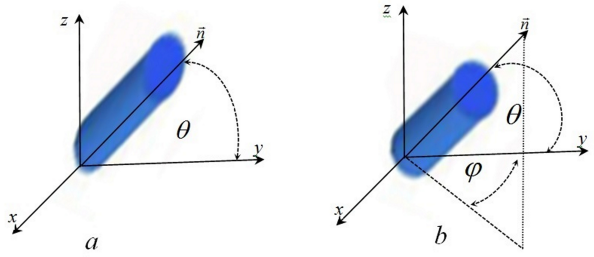

FIG. 5: LC director orientation in the LC element: a -in planar domain, b- in twist domain.

Considering that orthogonal polarized waves are not interfering, this element may be subdivided into two independent thin amplitude gratings with a rectangular groove profile for linearly polarized light horizontal and vertical directions of the E-vector (Fig. 7, b, c).

It is well known that the diffraction efficiency for a thin rectangular amplitude grating comes to $\eta_0 = 25$ % (zero-order diffraction - directly transmitted radiation) and $\eta_1 = 10.1\%$ (first-order diffraction) [39]. With due regard for diffractions from both gratings, the total signal is determined by a sum of the intensities of light beams diffracted from both gratings. Consequently, for directly transmitted radiation (zero order), the diffraction efficiency must amount to 50%, and in the case of the first-order diffraction - to 20.2%. The obtained values are in a good agreement with the experimental results given in Fig. 4 for voltages lower than the threshold. Note that the considered structure makes it possible to avoid such a limitation as 50%-loss for absorption as compared with the classical amplitude grating. Owing to this feature, one can have a twice as high diffracted signal in comparison to the typical amplitude grating.

4.2. Broken Mauguin mode: birefringence

Application of the control voltage leads to reorientation of the LC director and to the helix untwisting in a twist domain due to a change in

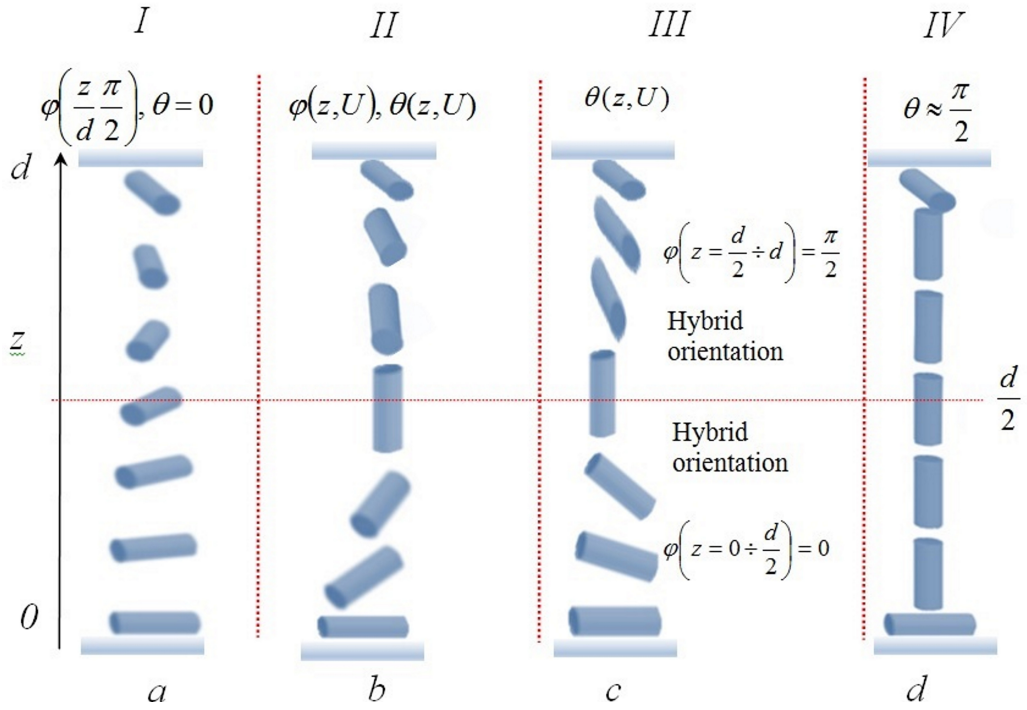

FIG. 6: Operating modes of the LC diffraction element: a - twist structure (polarization plane rotation); b - broken Mauguin mode (birefringence), c - hybrid orientation. In a half of the cell the director is within the vertical plane, whereas in the other half within the horizontal plane; d - homeotropic orientation of LC.

its polar θ and azimuthal ϕ angles. When the control voltage is as high as U = 1.5 V and is associated with the broken Mauguin mode [38], the E-vector of an electromagnetic wave fails to follow the director rotation and a domain with the twist structure exhibits birefringence (Fig. 6, b). Because of birefringence, the diffraction element begins to reveal the properties of a thin phase diffraction grating with higher diffraction efficiency.

4.3. Hybrid orientation

When the control signal is about 3V, the twist structure rotates with respect to the azimuthal angle ϕ and the situation is so that in one half of the cell (in depth of a LC layer) the director orientation is determined by the polar angle θ within the YZ plane, whereas in the other half - by the azimuthal angle ϕ within the XZ plane (Fig. 6, c). A twist domain no longer changes polarization state of the input beam. As seen in Fig. 4, the diffraction efficiency is at maximum approaching $\eta_1 = 28\%$ when the control voltage U = 3 V. A maximal value of the diffraction efficiency indicates that a rectangular profile of the grating grooves is transformed to the profile close to the sinusoidal one, with a maximal diffraction efficiency of 33.9 %.

4.4. Homeotropic orientation of LC

A further increase in the control voltage amplitude leads to reorientation of the LC director in planar and twist domains up to the polar angle $\theta = \frac{\pi}{2}$, and for voltages above 10 V the director orientation over the whole LC layer is close to the homeotropic orientation, leading to disappearance of the diffraction structure.

A theoretical analysis of the relationship

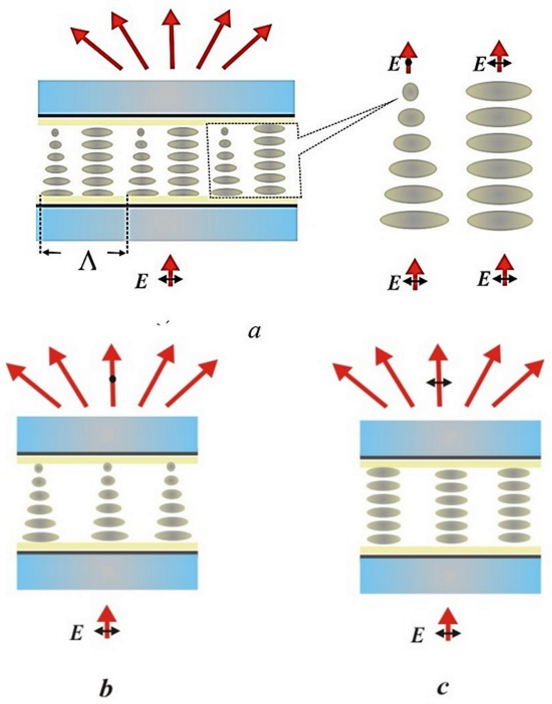

FIG. 7: (color online) Model of an amplitude diffraction grating.

between diffraction efficiency and control voltage is conducted in the approximation of a thin diffraction grating. The diffraction efficiency for the zero-order η_0 and the first-order η_1 diffraction is given by the following expression [40]:

$$\eta_0 = \cos^2 \frac{\Delta\phi}{2}, \tag{1}$$

$$\eta_1 = \frac{4}{\pi^2} \sin^2 \left(\frac{\Delta\phi}{2} \right), \tag{2}$$

where $\Delta\phi$ phase retardation.

Considering that for horizontally polarized light in a planar domain an extraordinary wave is excited, the phase retardation of light transmitted through the LC structure [33] may be written as:

$$\Delta\phi\,(U) = \frac{2\pi}{\lambda} d \left(\langle n_{ef_1}\,(\theta_p) \rangle - \left\langle n_{ef_2}\,(\theta_t, \phi) \right\rangle \right), \tag{3}$$

where $\langle n_{ef_1}\,(\theta_p) \rangle$ is the average effective absorption factor for a planar domain, $\left\langle n_{ef_2}\,(\theta_t, \phi) \right\rangle$ is the average effective refractive index for a twist domain when the Mauguin condition is broken, θ_p is the polar angle for a planar domain, θ_t is the polar angle for a twist domain, ϕ is the azimuthal angle for a twist domain.

The effective refractive index $\langle n_{ef_1}\,(\theta_p) \rangle$ for this light-propagation geometry in a planar domain is determined by the following expression:

$$\langle n_{ef_1}(\theta_p) \rangle = \frac{1}{d} \int_0^d n_{ef_1}(\theta_p(z)) dz, \tag{4}$$

where $n_{ef1}(\theta_p, Z) = \frac{n_o n_e}{\sqrt{n_o^2 \cos^2\theta_p(Z) + n_e^2 \sin^2\theta_p(Z)}}$ is the effective refractive index for horizontally polarized light in a planar domain.

The average effective refractive index for a twist domain $\left\langle n_{ef_2}\,(\theta_t, \phi) \right\rangle$ may be written as follows:

$$\left\langle n_{ef_2}(\theta_t, \phi\ )\right\rangle = \frac{1}{d}\int_0^d n_{ef_2}(\theta_t(Z), \phi(Z)\ )\mathrm{d}z, \quad (5)$$

where $n_{ef_2}(\theta_t(Z), \phi(Z)\ ) = \frac{n_o n_{ef}(\theta_t, Z)}{\sqrt{n_o^2\cos^2\phi(Z) + n_{ef}^2(\theta_t, Z)\sin^2\phi(Z)}}$ and $n_{ef}(\theta_t, Z) = \frac{n_o n_e}{\sqrt{n_o^2\cos^2\theta_t(Z) + n_e^2\sin^2\theta_t(Z)}}$.

When light is polarized vertically, the phase retardation $\Delta\phi$ is given by the expression

$$\Delta\phi = \frac{2\pi}{\lambda} d\left(n_o - \left\langle n_{ef_2}\left(\theta_t, \phi\right)\right\rangle\right), \quad (6)$$

where n_o is the refractive index for an ordinary wave characterizing the propagation rate of vertically polarized light in a planar domain.

The average effective refractive index for a twist domain $\left\langle n_{ef_2}\left(\theta_t, \phi\right)\right\rangle$ is determined by expression (5) due to symmetry of the problem.

To find the relationships for the planar angles $\theta_p(U)$, $\theta_t(U)$ and for the azimuthal angle $\phi(U)$, the authors have determined the coefficients of elasticity K11 and K33 for the nematic LC used, the initial LC director angle θ_0, permittivities along the and perpendicular to the director $\epsilon_{\|}$ and $\epsilon_{\perp}$, and the LC layer thickness d. The above parameters were calculated on the basis of comparison between the experimental and theoretical curves for transmission in a planar oriented LC cell at crossed polarizers as a function of the applied voltage at the wavelength λ =632.8 nm.

Transmission curves of the planar and twist structures at crossed polarizers as a function of the external voltage have been calculated with the use of a matrix model (Berryman matrix method [41]). Fig. 8 shows the transmission of a planar LC structure as a function of the applied control voltage.

As seen, by adequate fitting of the LC layer parameters, the authors have attained a good agreement between the experimental data and the results of numerical simulation. Table 1 presents the physical parameters determined by the numerical method, LC layer thickness and its initial angle for molecules within the cell.

Table 1: Parameters of LC cell used for numerical simulation.

d	$21.1\mu m$
K_{11}	$810^{-12}N$
K_{22}	$5\cdot10^{-12}N$
K_{33}	$10.8\cdot10^{-12}N$
K_{33}/K_{11}	1.35
θ_0	0.5^o
$\varepsilon_{\|}$	14.4
$\varepsilon_{\perp}$	5.60
n_o	1.534
n_e	1.690
Δn	0.156
λ	632.8 nm

The threshold values of the S-effect in the planar U_{tp} and in the twist U_{tt} domain, calculated proceeding from the LC cell parameters (Table 1), are slightly different: $U_{tp} = \pi\sqrt{\frac{k_{11}}{\varepsilon_0\Delta\varepsilon}} = 1.007\,V$, $U_{tt} = \pi\sqrt{\frac{K_{11}+(K_{33}-2K_{22})/4}{\varepsilon_0\Delta\varepsilon}} = 1.019\,V$.

To calculate the relationship between diffraction efficiency and control voltage, the LC director orientation angles has been determined as a function of the applied electric-field amplitude for the twist and planar structures $\theta_t(U, Z)\phi(U, Z)$, $\theta_p(U, Z)$. Calculations of the LC director orientation in an external electric field have been conducted using the algorithm for minimization of the total free energy of a LC system in the vector representation for a field of the director $\vec{n}$ [42, 43]. The method of finite differences in a rectangular mesh was used [44].

Fig. 9 demonstrates the calculated

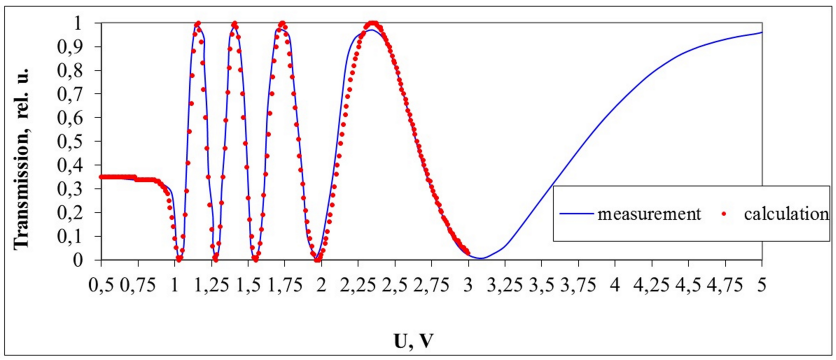

FIG. 8: (color online) Transmission of a planar LC cell at crossed polarizers as a function of the control voltage.

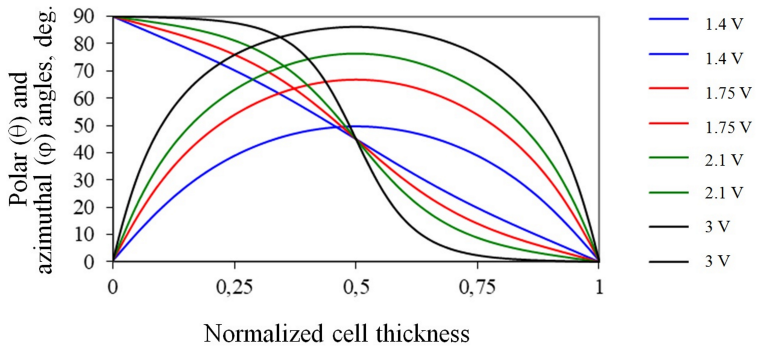

FIG. 9: (color online) Distribution of the angles and in depth of the cell for different working voltages at the twist-effect.

distribution plot for the polar angle $\theta_t(U, Z)$ and the azimuthal angle $\phi(U, Z)$ of the director orientation in depth of the cell at different operating-voltage amplitudes in a twist domain.

The obtained results demonstrate that a threshold value of the twist-effect voltage (broken Mauguin condition) is at a level of the voltage amplitude about $U = 1.5\ V$. When voltages are higher than $U = 3\ V$, the hybrid orientational mode is observed.

Fig. 10 shows the calculated curves for the LC director orientation angle as a function of the voltage applied to the LC layer for planar $(\theta_p(U, \frac{d}{2}))$and twist $\theta_t(U, \frac{d}{2}))$ domains.

The calculated curves in Fig. 10 point to the fact that close to the S-effect threshold voltage (over the range 0.8 – 1.2 V) a planar domain is switched faster, then advance of the director reorientation in a twist domain takes place. When voltages are higher than 5 V, the polar director-orientation angles for the planar and twist domains are equated and go to saturation (homeotropic orientation).

Fig. 11 presents the calculated plot for the transmission of a twist structure at crossed polarizers as a function of the applied voltage.

The results of mathematical modeling shown in Figs. 9 – 11 point to the fact that Mauguin's condition for the twist structure is broken at the voltage U=1.5 V. When voltages are higher than 3 V, the twist structure leaves polarization of light transmitted through the LC element unaltered (hybrid or homeotropic orientation of the director). In the range of voltages U = 1.5–3

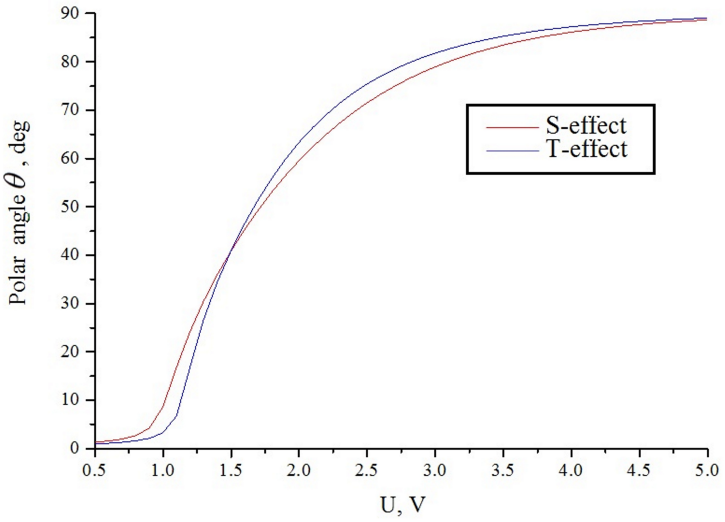

FIG. 10: (color online) Polar angle on center of the cell as a function of the applied voltage: S-effect: initial planar orientation; T-effect: initial twisted (90°) orientation.

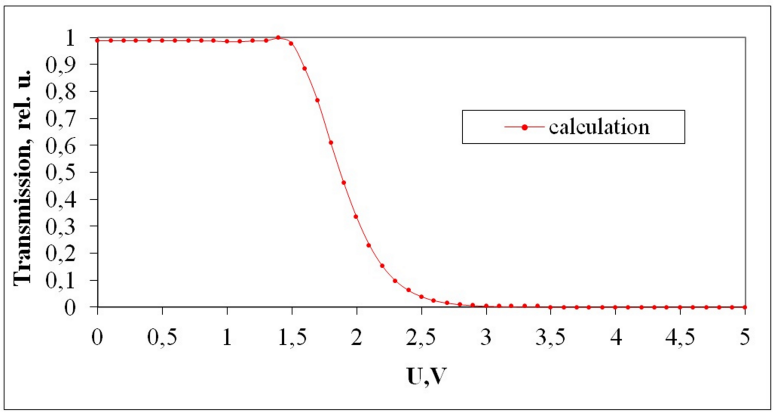

FIG. 11: (color online) Transmission of the twist cell at crossed polarizers as a function of the applied voltage.

V the twist structure deformed by an electric field ceases to exhibit the optical activity and begins to reveal birefringence. This results in excitation in a twist domain of the polarization mode having the polarization vector coincident with that of the wave transmitted through a planar domain. At 3 V the twist structure begins to exhibit the hybrid orientational mode when in one half of the cell the LC director is within the vertical plane and in the other half - within the horizontal plane of the LC element. At such orientation of LC, the propagation rate of the polarization modes under study in a twist domain is characterized by the refractive indices n_o and n_e which interchange their places when reaching a half of the LC layer depth $(d/2)$.

Based on the performed numerical simulation using formulae $(1-6)$, the diffraction efficiency has been calculated as a function of the applied voltage for zero- and first-order

diffractions (Fig. 12).

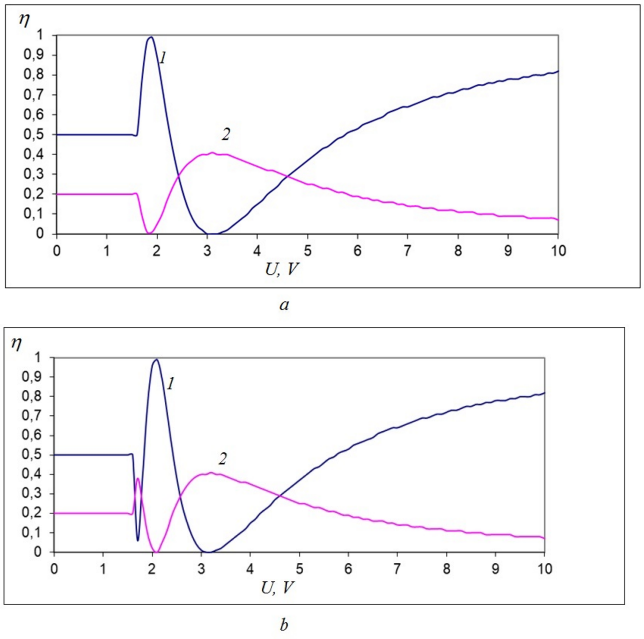

FIG. 12: (color online) Calculated curves for diffraction efficiency as a function of voltage at vertical (a) and horizontal (b) polarizations of input radiation: 1 – zero-order diffraction, 2 – first-order diffraction.

The plots have been constructed with the use of the diffraction efficiencies corresponding to the experimental data in the mode of diffraction from the amplitude grating (Fig. 4).

As demonstrated by the results of analytical calculations, the inclusion of the differences in parameters for the Fredericks transition in planar and twist domains results in a good qualitative agreement between the experimental and theoretical results for the dependence of diffraction efficiency on control voltage.

5. Analysis of polarization states

Fig. 13 shows the experimental results for polarization states of directly transmitted light (zero-order diffraction) and of light transmitted in the direction of the first diffraction maximum at vertical polarization of light incident on the grating. The measurements were performed at different control voltages.

As demonstrated by the results (Fig. 13), when no voltage is applied, polarization of light propagating in the directions of zero-order and first-order diffractions changes with respect to polarization of incident radiation. Light becomes elliptically polarized. As this takes place, the orientation of the major axes of polarization ellipses relative to the vector for light incident on the LC element makes the angles close to $+45^{\circ}$ for 0 – order diffraction and 45° for 1 – order diffraction, respectively. Changing of the polarization state is associated with the phase retardation determined by the difference in refractive indices. As the control voltage is applied, the polarization state of diffracted light is changed.

Using the theoretically derived dependencies for the polar and azimuthal director orientations at different control voltages, the authors have analyzed polarization states of radiation transmitted in the direction of the zero-order and first-order diffraction maxima. Polarization states of light are described using the Jones matrix formalism [45]. The diffraction element in a one half of the diffraction structure period from $-\frac{\Lambda}{2}$ to 0 represents a planar structure and in the other half from 0 to $\frac{\Lambda}{2}$ represent a twist one. Let us express the amplitude $E(m)$ of diffracted components at the m-order diffraction as a Fourier image of the grating transmission factor [48]:

$$E(m) = \frac{1}{\Lambda}\int\limits_{-\frac{\Lambda}{2}}^{0} T_{pl}\exp\left(\frac{2\pi imx}{\Lambda}\right)dx + \frac{1}{\Lambda}\int\limits_{0}^{\frac{\Lambda}{2}} T_{tw}\exp\left(\frac{2\pi imx}{\Lambda}\right)dx, \qquad (7)$$

where T_{pl} is the Jones matrix for the planar structure, T_{tw} is the Jones matrix for the twist structure.

For a planar domain, the Jones matrix is of the form [47]:

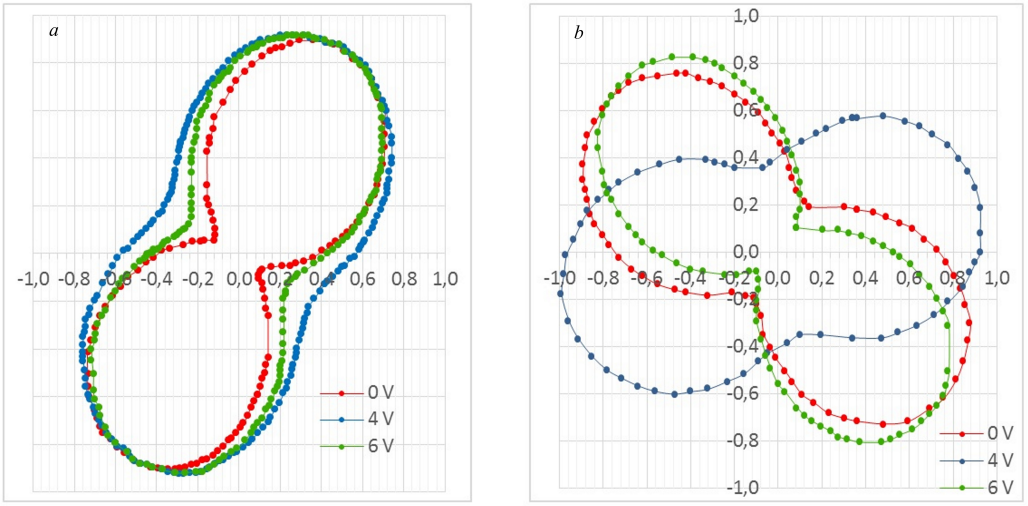

FIG. 13: (color online) Polarization diagrams for light transmitted through the LC cell at different control voltages: (a) zero-order diffraction, (b) first-order diffraction.

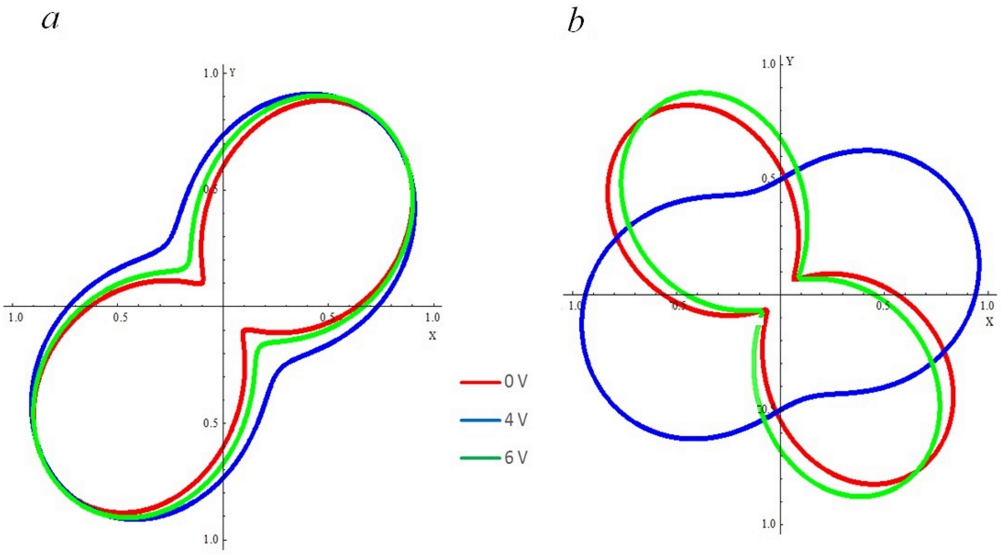

FIG. 14: (color online) Polarization diagram of diffracted light at (a) zero-order diffraction and (b) first-order diffraction.

$$T_{pl} = \begin{pmatrix} \exp\dfrac{i\,2\pi d\Delta n}{\lambda} & 0 \\ 0 & \exp\dfrac{-i\,2\pi d\Delta n}{\lambda} \end{pmatrix}, \quad (8)$$

where d is the LC cell thickness, Δn is LC anisotropy, λ is the radiation wave length.

For the twist structure, the Jones matrix is given as follows [46]:

$$T_{tw} = \begin{pmatrix} a - ib & -c - if \\ c - if & a + ib \end{pmatrix} \quad (9)$$

with the coefficients

$$a = \cos\phi\cos\chi + \frac{\phi}{\chi}\sin\phi\sin\chi,\ b = \frac{\delta}{\chi}\cos\phi\sin\chi,$$
$$c = \sin\phi\cos\chi - \frac{\phi}{\chi}\cos\phi\sin\chi,\ f = \frac{\delta}{\chi}\sin\phi\sin\chi,$$
$$\delta = \frac{\pi d\left(n_{ef}\left(\theta_t\right) - n_o\right)}{\lambda},\ \chi^2 = \phi^2 + \delta^2.$$

Using the Jones vector for the vertically polarized light that enters the element and the Jones matrix for a polarizer [49], we can have the Jones vector describing polarization of light at the output of a system (LC cell, polarizer):

$$E_{out}(m) = \begin{pmatrix} \cos^2\alpha & \sin\alpha\cos\alpha \\ \sin\alpha\cos\alpha & \sin^2\alpha \end{pmatrix} \left(\frac{1}{\Lambda}\int\limits_{-\frac{\Lambda}{2}}^{0} T_{pl}\exp\left(\frac{2\pi i m x}{\Lambda}\right)dx + \frac{1}{\Lambda}\int\limits_{0}^{\frac{\Lambda}{2}} T_{tw}\exp\left(\frac{2\pi i m x}{\Lambda}\right)dx \right) \begin{pmatrix} 0 \\ 1 \end{pmatrix} \tag{10}$$

where α is the angle between the polarizer transmission-plane direction and the OZ axis.

Fig. 14 presents the calculated polarization diagrams for light transmitted in the direction of the diffraction orders $m = 0$ and $m = 1$ for the LC director orientation angles coincident with the experimental parameters given in Fig. 13.

In Figs. 13 and 14 it is seen that the theoretical results for polarization states of light diffracted from the LC element are in a good agreement with the experimental results, pointing to correctness of the parameters determined for the Fredericks transition in different domains of the LC structure which were used to estimate the effective refractive indices in planar and twist domains of the structure.

In this way the theoretical and experimental studies considered in this paper allow for analysis of the features of light diffraction from the twist or planar electrically-controlled diffraction structure, demonstrating that polarization is dependent on the voltage applied to the LC cell.

6. Discussion and conclusion

It may be concluded that the conducted experimental and theoretical studies make it possible to analyze the features of light diffraction from the twist-planar electrically controlled diffraction structure. It is revealed that at minor voltages (1.5 V) the diffraction structure may be considered as a combination of two amplitude gratings with orthogonal polarizations at the output. When the voltage applied to the LC element is increased up to the value associated with the broken Mauguin condition (optical threshold of the twist effect), the amplitude-to-phase transformation of the diffraction structure is the case and diffraction efficiency becomes higher. Maximal diffraction efficiency for the first-order diffraction is about 28% (at the voltage 3V), approaching the limiting value of diffraction efficiency for a thin sinusoidal phase grating. Further increase of voltages leads to reorientation of the LC director within planar and twist domains, whereas at voltages above 10 V the director orientation is close to homeotropic over the whole LC layer volume and the diffraction structure disappears.

It has been found that diffraction characteristics of the LC elements are dependent on polarization of incident light. This has been explained using the theoretical model developed on the basis of calculations for the dependence of polar and azimuthal angles of the LC director orientation in planar and twist domains on the control voltage. A theoretical analysis of the relationship between diffraction

efficiency and voltage has been performed for two orthogonal polarization modes. Using the Jones matrix method, the authors have analyzed the diffracted-radiation polarization states as a function of the control voltage.

It should be noted that the proposed LC elements are characterized by high diffraction efficiency and have considerable promise in the development of control systems for laser beams owing to the electric control of the light-beam intensity and polarization at diffraction of different orders.

References

[1] V.G. Chigrinov. *Liquid crystal photonics: engineering tools, techniques and tables.* (Nova Science Publishers, New York, 2014).

[2] H.S. Kwok. *Progress in Liquid Crystal Science and Technology.* (World Scientific Publishing Company, Singapore, 2013).

[3] T.H. Lin, A.Y.-G. Fuh. Polarization controllable spatial filter based on azo-dye-doped liquid-crystal film. Opt. Lett. **30**, 1390 (2005).

[4] Z. He, F. Gou, R. Chen, K. Yin, T. Zhan, S.-T. Wu, Liquid crystal beam steering devices: principles, recent advances, and future developments. Cryst. **9**, 292 (2019).

[5] D. Lee, H. Lee, L.K. Migara, K. Kwak, V. P. Panov, J.-K. Song. Widely tunable optical vortex array generator based on grid patterned liquid Crystal Cell. Adv. Opt. Mater. **9**, 2001604 (2021).

[6] I. Nys, J. Beeckman, K. Neyts. Fringe-field-induced out-of-plane reorientation in vertically aligned nematic spatial light modulators and its effect on light diffraction. Liq. Cryst. **40**, 1516 (2021).

[7] H. Sarkissian, S.V. Serak, N.V. Tabiryan et al. Polarization-controlled switching between diffraction orders in transverse-periodically aligned nematic liquid crystals. Opt. Lett. **31**, 2248 (2006).

[8] M. Bouvier and T. Scharf. Analysis of nematic liquid crystal binary gratings with high spatial frequency. Opt. Eng. **39**, 2129 (2000).

[9] M. Honma and T. Nose. Temperature-independent achromatic liquid-crystal grating with spatially distributed twisted-nematic orientation. Appl. Phys. Express **5**, 062501 (2012).

[10] S. Valyukh, V. Chigrinov, H. S. Kwok, H. Arwin. On liquid crystal diffractive optical elements utilizing inhomogeneous alignment. Opt. Express **20**, 15209 (2012).

[11] K.A. Rutkowska, M. Chychlowski, M. Kwasny, I. Ostromecka, J. Pilka, U.A. Laudyn. Light propagation in periodic photonic structures formed by photo-orientation and photo-polymerization of nematic liquid crystals. Opto-Electron. Rev. **25**, 118 (2017).

[12] M. Nieborek, K. Rutkowska; T.R. Wolinski; B. Bartosewicz, B. Jankiewicz, D. Szmigiel, A. Kozanecka-Szmigiel. Tunable Polarization Gratings Based on Nematic Liquid Crystal Mixtures Photoaligned with Azo Polymer-Coated Substrates. Cryst. **10**, 768 (2020).

[13] K. Takatoh. *Alignment Technologies and Applications of Liquid Crystals.* (Taylor and Francis Group, London and New York, 2014).

[14] P.T. Mather. *Advances in liquid crystalline materials and technologies.* Volume **709** (MRS Proceedings) (Cambridge University, London, 2014).

[15] O. Yaroshchuk and Yu. Reznikov. Photoalignment of liquid crystals: basics and current trends. Jour. Mater. Chem. **22**, 286 (2012).

[16] B. Lochab, M. Monisha; N. Amarnath; P. Sharma; S. Mukherjee; H. Ishida. Review on the accelerated and low-temperature polymerization of benzoxazine resins: addition polymerizable sustainable polymers. Polymers **13**, 1260 (2021).

[17] I. Valyukh, H. Arwin, V. Chigrinov, S. Valyukh. UV-induced in-plane anisotropy in layers of mixture of the azo-dyes SD-1/SDA-2 characterized by spectroscopic ellipsometry. Physica Status Solidi (C) **5**, 1274 (2008).

[18] S. Valyukh, I. Valyukh, V. Chigrinov, H.S. Kwok, H. Arwin. Liquid crystal light deflecting devices based on nonuniform anchoring. Appl. Phys. Let. **97**, 231120 (2010).

[19] U. Mahilny, A. Stankevich, A. Trofimova. Liquid crystal monomer alignment by polymers with benzaldehyde groups. Vestnik BSU. Ser. Phys.

Math. Inform. **1**(2), 17 (2014). (in Russian)

[20] U. Mahilny, A. Trofimova, A. Stankevich, A. Tolstik, A. Murauski, A. Muravsky. New photocrosslinking polymeric materials for liquid crystal photoalignment. Int. J. Nonlinear Phenomena in Complex Systems **16**, 79 (2013).

[21] I. Fujieda. Liquid-crystal phase grating based on in-plane switching. Appl. Opt. **40**, 6252 (2001).

[22] J.H. Park, Ch.J. Yu, J. Kim, S.Y. Chung, S.D. Lee. Concept of a liquid-crystal polarization beamsplitter based on binary phase gratings. Appl. Phys. Lett. **83**, 1918 (2003).

[23] V. Presnyakov, K. Asatryan, T. Galstian, and V. Chigrinov. Optical polarization grating induced liquid crystal micro-structure using azo-dye command layer. Opt. Express **14**, 10558 (2006).

[24] H. Chen, G. Tan, Y. Huang, Y. Weng, T.-H. Choi, T.-H. Yoon, S.-T. Wu. A Low Voltage Liquid Crystal Phase Grating with Switchable Diffraction Angles. Sci. Rep. **7**, 39923 (2017).

[25] M. Honma, T. Nose. Twisted nematic liquid crystal polarization grating with the handedness conservation of a circularly polarized state. Opt. Express **20**, 18449 (2012).

[26] S.V. Serak, D.E. Roberts, J.Y. Hwang, S.R. Nersisyan, N.V. Tabiryan, T.J. Bunning, D.M. Steeves, B.R. Kimball. Diffractive waveplate arrays. J. Opt. Soc. Am. B **34**, B56 (2017).

[27] K. Kawai, T. Sasaki, K. Noda, M. Sakamoto, M.; N. Kawatsuki, H. Ono. Holographic binary grating liquid crystal cells fabricated by one-step exposure of photocrosslinkable polymer liquid crystalline alignment substrates to a polarization interference ultraviolet beam. Appl. Opt. **54**, 6010 (2015).

[28] Y. Weng, D. Xu, Y. Zhang, X. Li, S.T. Wu. Polarization volume grating with high efficiency and large diffraction angle. Opt. Express **24**, 17746 (2016).

[29] S. Y. Huang, S. T. Wu, A. Y. G. Fuh. Optically switchable twist nematic grating based on a dye-doped liquid crystal film. Appl. Phys. Lett. **88**, P.041104 (2006).

[30] V. Kapoustine, A. Kazakevitch, V. So, R. Tam. Simple method of formation of switchable liquid crystal gratings by introducing periodic photoalignment pattern into liquid crystal cell. Opt. Commun. **266**, 1 (2006).

[31] W. Y. Wu, A. Y. G. Fuh. Rewritable liquid crystal gratings fabricated using photoalignment effect in dye-doped poly(vinyl alcohol) film. Jpn. J. Appl. Phys. **46**, 6761 (2007).

[32] W. Hu, A. Srivastava, F. Xu, J.-T. Sun, X.-W. Lin, H.-Q. Cui, V. Chigrinov, Y.-Q. Lu. Liquid crystal gratings based on alternate TN and PA photoalignment. Opt. Express **20**, 5384 (2012).

[33] R. Weglowski, A. Kozanecka-Szmigiel, W. Piecek, J. Konieczkowska, E. Schab-Balcerzak. Electro-optically tunable diffraction grating with photoaligned liquid crystals. Opt. Commun. **400**, 144 (2017).

[34] A. A. Kazak, E. A. Melnikova, A. L. Tolstik, U. V. Mahilny, A. I. Stankevich. Controlled diffraction liquid-crystal structures with a photoalignment polymer. Tech. Phys. Lett. **34**, 861 (2008).

[35] A.A. Kazak, A.L. Tolstik, E.A.Melnikova, A.A. Komar. Operation with laser radiation by using of liquid crystal elements. Nonlinear Phenomena in Complex Systems **16**, 302 (2013).

[36] A.A. Kazak, E.A. Melnikova, O.G. Romanov, A.L. Tolstik. Formation of singular and Bessel light beams using electrically controlled liquid crystal diffractive elements. Int. J. Nonlinear Phenomena in Complex Systems **18**, 170 (2015).

[37] U. V. Mahilny, A I Stankevich, A A Muravsky, A A Murauski. Novel polymer as liquid crystal alignment material for plastic substrates, J. Phys. D. Appl. Phys. **42**, 075303 (2009).

[38] C.V. Mauguin. Sur les cristaux liquides de Lehman. Bull. Soc. Fr. Miner. **34**, 71 (1911).

[39] R. J. Collier, C. B. Burckard, L. H. Lin. *Optical Holography.* (Academic Press New York and London, New Jersey, 1971).

[40] J.E. Goodman. *Introduction to Fourier Optics.* (McGraw-Hill, New York, 2nd ed., 1996).

[41] D.W.Berreman. Optics in stratified and anisotropic media: 4 x 4-matrix formulation. J. Opt.Soc.Am. **62**, 502 (1972).

[42] L.M. Blinov. *Liquid crystals. Structure and properties.* (URSS, 2018).

[43] B.E.A. Saleh, M.C. Teich. *Fundamentals of Photonics.* (Hoboken,Wiley, 2nd ed. 2007).

[44] H. P. Langtangen, S. Linge. *Finite Difference Computing with PDEs. A Modern Software Approach.* (Springer, Cham, 2017).

[45] A. Trofimova, U. Mahilny. Anisotropic gratings based on patterned photoalignment of reactive mesogen. J. Opt. Soc. Am. **31**, 948 (2014).

[46] R. C. Jones. A new calculus for the treatment of optical systems V. A More General Formulation, and Description of Another Calculus. J. Opt. Soc. Am. **37**, 107 (1947).

[47] A. Gerrard, J.M. Bürch. *Introduction to Matrix Methods in Optics.* (Wiley) 1975.